Liquid Crystal Polymers Containing Macroheterocyclic Ligands. 5.† Structure of the Liquid Crystal Phases of Poly[4-[(11-methacryloylundecan-1-yl)oxy]-4'-(4'-carboxybenzo-15-crown-5)biphenyl]

G. Ungar*

School of Materials, The University of Sheffield, Sheffield S10 2TZ, U.K.

V. Percec* and R. Rodenhouse

Department of Macromolecular Science, Case Western Reserve University, Cleveland, Ohio 44106

Received May 21, 1990; Revised Manuscript Received October 19, 1990

ABSTRACT: The liquid crystalline phases displayed by poly[4-[(11-methacryloylundecan-1-yl)oxy]-4'-(4'-carboxybenzo-15-crown-5)biphenyl] were characterized by a combination of DSC, thermal optical polarized microscopy and X-ray scattering (WAXS and SAXS) techniques. All three techniques demonstrate that the polymer exhibits a nematic mesophase between 129 and 166 °C. DSC and thermal optical microscopy experiments suggest a single smectic phase below 129 °C. However, X-ray scattering experiments have demonstrated that three different smectic phases appear below the nematic phase: a high-temperature interdigitated monolayer S_A phase, which is stable between 132 °C and about 125 °C (layer periodicity L = 41 Å); a lower temperature unindentified smectic phase with layer periodicity L = 57 Å (probably a double-layer tilted phase that is stable up to 125 °C); and a metastable smectic C phase (layer periodicity L = 32 Å). The smectic C phase is kinetically favored over the phase with L = 57 Å. The bulkiness of the crown ether group and its specific interactions cause a series of unusual behaviors as, for example, a very low rate of transformation of the smectic A and of the smectic phase with L = 57 Å and a highly discontinuous smectic C to smectic A phase transition. The influence of sample history on the interconversion of these phases is presented. Two possible molecular models for the smectic A phase are discussed.

Introduction

We are investigating the synthesis of liquid crystalline polymers containing macroheterocyclic ligands. Liquid crystalline macroheterocyclic ligands may add a new dimension to the field of host–guest chemistry that to date was performed either in an isotropic solution or in a three-dimensional crystalline phase. These polymers should be capable of forming mesomorphic host–guest complexes, which could provide a new approach to systems that combine selective recognition with external regulation.[1-3]

To date there are only a few classes of low molar mass liquid crystals containing macroheterocyclic ligands. The first refers to a series of benzo-15-crown-5 and azacrown ether derivatives containing biphenyl or cholesteryl mesogenic units.[4-6] These compounds display calamitic mesophases. The second refers to several substituted azacrown derivatives, which display columnar or tubular mesophases.[7,8]

The insertion of crown ethers into the structure of a liquid crystalline polymer has been accomplished in three ways. First, the macroheterocyclic ligand was incorporated into a main-chain liquid crystalline polymer through the polyetherification of a macroheterocyclic bis-electrophile with a mesogenic bisphenol.[9] Second, the ligand was incorporated into a side-chain liquid crystalline polymer by the synthesis of a monomer containing a macroheterocyclic ligand as an intregal part of the mesogenic unit.[10,11] Third, cyclocopolymerization of α,ω-divinyl ethers of ethylene glycols with a vinyl ether containing a mesogenic side group led to liquid crystalline polymers that contain crown ether structural units within the polymeric backbone.[12] Similarly, cyclopolymerization of α,ω-divinyl ethers of ethylene glycols that contain a mesogenic unit directly attached to this polymerizable group led to homopolymers with mesomorphic behavior.[13]

Side-chain liquid crystalline polymers containing these types of macroheterocyclic ligands are of interest for potential application in ionic channel forming devices that may be turned on and off by some sort of external thermal, electric, or magnetic regulation. In order to investigate these areas we must first understand the structural arrangement of the polymer side groups in its different liquid crystalline states. Therefore, X-ray scattering experiments have been performed in order to further characterize the mesophases, which to date have been identified by a combination of differential scanning calorimetry and optical polarized microscopy.

This paper discusses the first X-ray scattering studies of the side chain liquid crystalline polymethacrylate containing 4-(11-undecan-1-yloxy)-4'-(4'-carboxybenzo-15-crown-5)biphenyl side groups.[10]

Experimental Section

Materials. Poly[4-[(11-methacryloylundecan-1-yl)oxy]-4'-(4'-carboxybenzo-15-crown-5)biphenyl] (PMC-11) was synthesized as previously reported.[10] M_n = 14 600; M_w/M_n = 2.8. The structure of this polymer is given in Chart I.

Techniques. X-ray scattering patterns were recorded with either a flat plate wide angle (WAXS) vacuum camera (room temperature and elevated temperatures) or a pinhole collinated small-angle (SAXS) camera (room temperature). Ni-filtered Cu Kα radiation was used. The samples were in the form of (a) fibers pulled from the melt, (b) bulk samples in Lindemann capillaries cooled from the melt, or (c) as-prepared polymers in the form of a free standing powder. The temperature stability of the X-ray heating cell was ±0.1 °C. Thermal transitions and thermodynamic parameters were determined by using a Perkin-Elmer DSC-4 differential scanning calorimeter equipped with a

† Previous paper in this series: ref 12.

0024-9297/91/2224-1996$02.50/0

Chart I
Structure of Poly[4-[(11-methacryloylundecan-1-yl)-oxy]-4'-(4'-carboxybenzo-15-crown-5)biphenyl] (PMC-11)

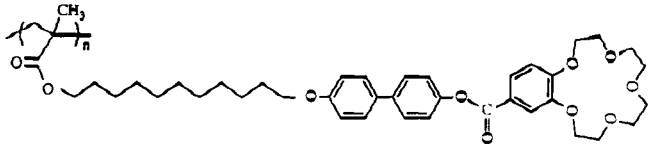

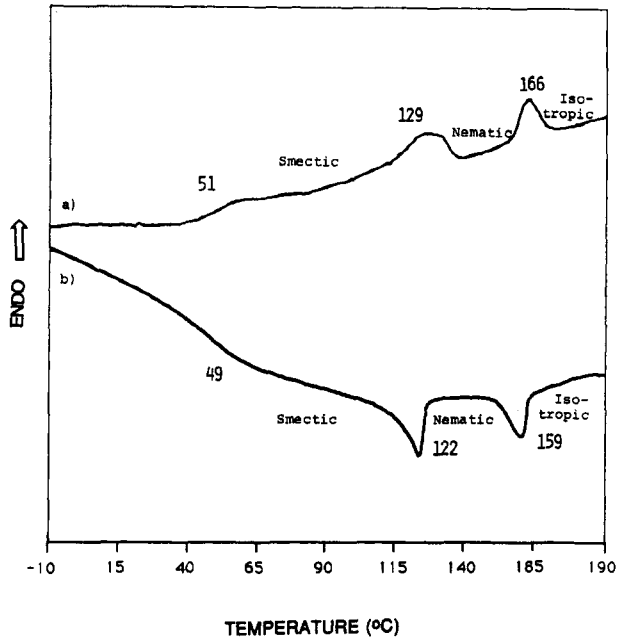

Figure 1. Heating (a) and cooling (b) DSC traces of PMC-11 (20 °C/min).

TADS 3600 data station. Heating and cooling rates were 20 °C/min. A Carl Zeiss optical polarized microscope (magnification 100×) equipped with a Mettler FP 82 hot stage and a Mettler FP 80 central processor was used to observe the thermal transitions and to analyze the anisotropic textures.

Results and Discussion

DSC Results. The heating and cooling DSC traces of PMC-11 are presented in Figure 1 together with the assignment of the mesomorphic phase transitions as described in a previous publication.[10]

Molecular Model. Bond lengths, bond angles, and torsion angles used for modeling the PMC-11 monomer unit were taken from different literature sources. Data for the benzocrown moiety were taken from the crystallographic study of the uncomplexed compound by Hanson.[14] The remaining portion of the side chain was modeled by using the data in refs 15–18. Figure 2 shows what is believed to be the minimum-energy conformation of the monomer repeat unit. The length of the extended unit, including the van der Waals radii, is 41 Å.

X-ray Scattering Results of the Nematic Phase. The X-ray scattering pattern of the polymer PMC-11 recorded in the temperature range between the two endotherms at 129 and 166 °C contains no sharp rings. Figure 3 shows a densitometer trace of a scattering pattern from the bulk specimen of PMC-11 recorded at 148 °C. The main feature is the diffuse maximum of $Q = 1.4$ Å^{-1} ($Q = 4\pi \sin\theta/\lambda$). Note that the other broad halo around $Q = 0.50$ Å^{-1} is mainly due to the scattering on the capillary. Since the polymer in this temperature range is optically anisotropic (Figure 4), it is concluded that the phase between the endotherms at 129 and 166 °C is nematic.

The as-prepared polymer, precipated from methanol, also gives only diffuse X-ray scattering, as seen in Figure 5, curve a. Since no glass capillary was used here, the low-angle diffuse peak ($Q \approx 0.4$ Å^{-1}) in Figure 5a is much weaker than that in Figure 3. Nevertheless, it is still present and is thus due to genuine scattering from the polymer. Since the solution-cast films of PMC-11 are optically anisotropic at room temperature, the phase is identified as nematic glass. Note that the glass transition temperature (T_g) of PMC-11 is at 50 °C, as determined by calorimetry (see Figure 1).

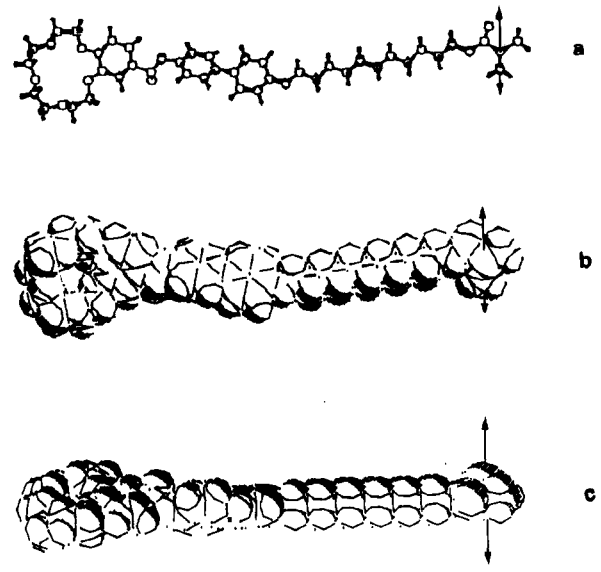

Figure 2. Minimum-energy model of a monomer repeat unit of PMC-11: (a) ball and stick; (b) space filling, flat on; (c) space filling, edge on. Arrows indicate extension of backbone.

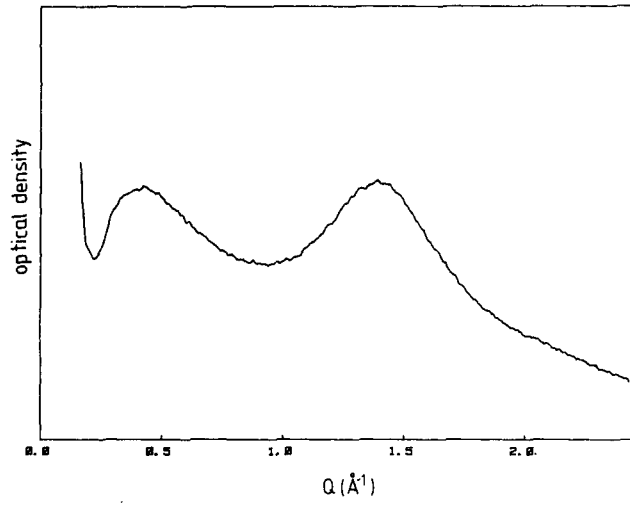

Figure 3. Radial photodensitometer scan of the scattering pattern of the PMC-11 in the nematic phase, recorded at 148 °C. The curve is the average of 360 radial scans separated by an azimuthal increment of 1°. The letter also applies to Figure 3.

X-ray Scattering Results of Smectic Phases. We now proceed with a description of the complex smectic phase behavior of PMC-11. When the nematic glass is heated to a temperature sufficiently above T_g, two additional rings appear in the low-angle diffraction region, corresponding to Bragg spacings of 57 and 19 Å. They are much sharper than the diffuse rings of the nematic phase but still considerably broader than those expected from well-developed smectics. With increasing annealing temperature the new peaks sharpen up somewhat, though not significantly. The densitometer trace of the sample annealed from the nematic glass at 110 °C is shown in Figure 5, curve b.

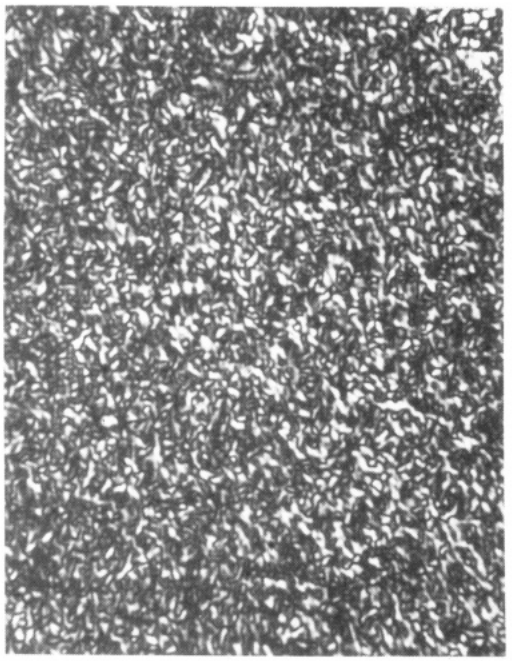

Figure 4. Optical polarized texture (100×) of the nematic mesophase of the polymer at 162 °C.

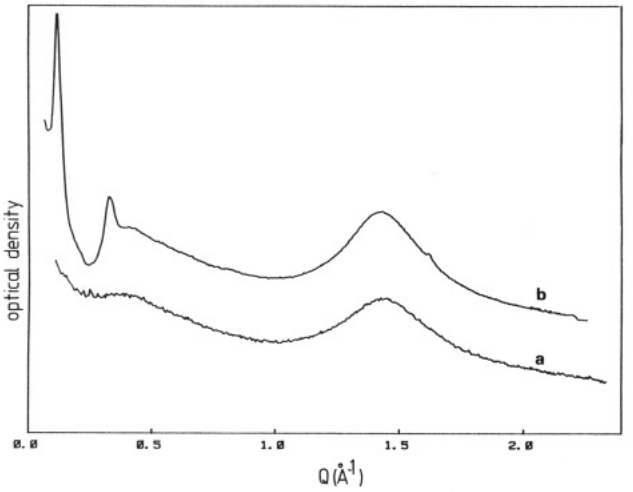

Figure 5. Radial photodensitometer scans of scattering patterns of PMC-11: (a) polymer precipatated from solution (nematic glass); (b) precipatated from solution and subsequently annealed at 110 °C (57-Å smectic phase).

Above 120 °C the 57-Å phase starts transforming into what will be referred to as the 41-Å phase. A ring corresponding to the Bragg spacing of 41 Å appears first at 120 °C, but above this temperature the viscosity drops markedly, so that free standing specimens are not easily studied. Figure 6 shows an X-ray scattering pattern of the pure 41-Å phase taken at 127 °C with the sample in a capillary (hence the intense diffuse inner ring). The 41-Å ring from the sample is strong and sharp. A weak second order (21 Å) is also discernible on the negative.

The 41-Å phase persists on cooling at least down to 113 °C. On further slow cooling to 90 °C (3 °C/h) an almost complete conversion back to the 57-Å phase takes place. The 57- and 19-Å reflections thus obtained are much sharper than those produced on annealing the nematic glass yet not as sharp as the 41-Å reflection. In addition to the 52- and 19-Å reflections, a weak and sharp reflection corresponding to a spacing of 32 Å is observed in the sample slowly cooled to 90 °C. The pattern remains unchanged on further cooling. A SAXS pattern obtained after cooling

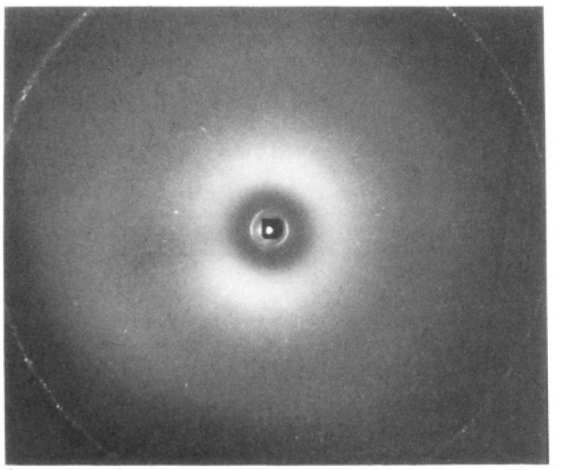

Figure 6. WAXS pattern of PMC-11 in a glass capillary, recorded at 127 °C (41-Å smectic phase). The sharp outer ring is due to calcite used for calibration.

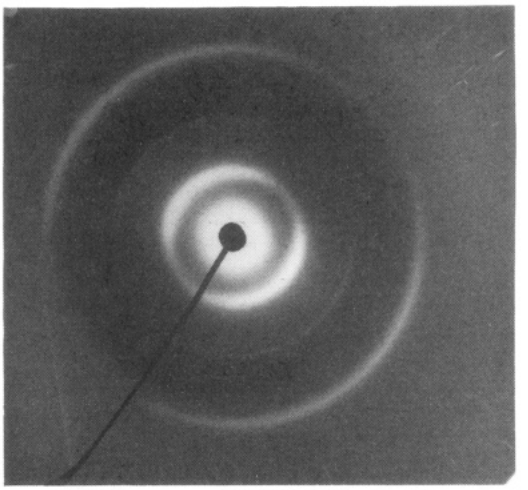

Figure 7. SAXS pattern of PMC-11 that had been heated to 127 °C, then slowly cooled to 90 °C, annealed at 90 °C, and subsequently cooled to room temperature (57-Å smectic phase; 001 and 003 reflections are visible; the weak sharp middle ring is due to a trace of the 32-Å smectic phase).

to room temperature is shown in Figure 7.

If instead of being slowly cooled from 113 °C the polymer is quenched, then the X-ray pattern subsequently recorded shows similar features as in Figure 5b or 7, except that the 32-Å ring is now selectively stronger and a second-order (16 Å) reflection is observed. The 57- and 19-Å rings in the quenched sample are broad, while the 32- and 16-Å ones are sharp. Thus a third smectic phase with layer spacing of 32 Å is present in addition to the 57-Å phase.

X-ray Scattering Experiments for Polymer Fiber. At room temperature melt-drawn fibers of PMC-11 usually contain both 32- and 57-Å smectic phases in varying proportions. Although the flowing melt is cooled rapidly during fiber drawing, the nematic phase has never been frozen in. This would indicate that shear promotes smectic ordering.

Figure 8 shows a typical SAXS pattern of a fiber. This particular fiber had been annealed at 80 °C after drawing, but there is no noticeable difference between this pattern and that of an as-drawn fiber. The very broad first- and third-order scattering maxima of the 57-Å phase are seen, as well as the sharp first-order reflection of the 32-Å phase. In this as in all other fibers the layer reflections are strictly equatorial, in compliance with the general rule that smectic layers tend to align parallel to the direction of shear.[19]

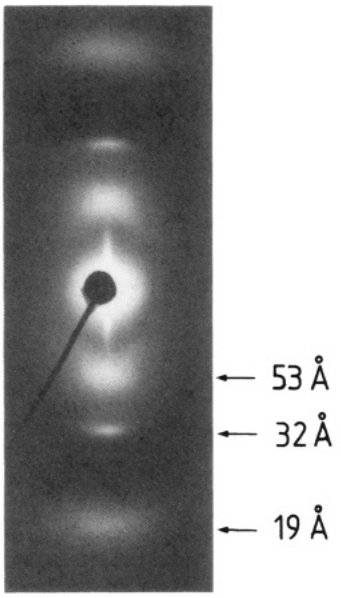

Figure 8. SAXS pattern of a PMC-11 melt-down fiber that had been annealed at 80 °C (57- and 32-Å smectic phases). Fiber axis is vertical.

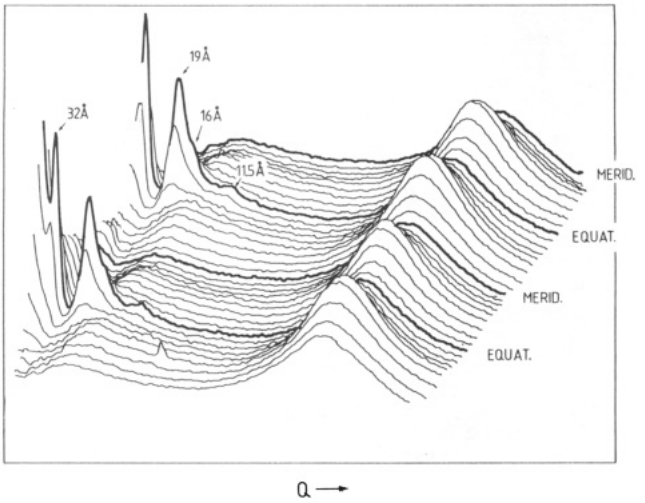

Figure 9. Series of radial photodensitometer traces of the WAXS pattern of an as-drawn fiber of PMC-11. The curves are separated by an azimuthal increment of 10°. Each trace is an average of 10 scans covering a ±4° sector. The predominant phase is the 57-Å smectic (003 at 19 Å, 005 at 11.5 Å) with the 32-Å phase as the minority component (001 at 32 Å, 002 at 16 Å).

While the orientational order of layers is high in both phases, the extreme breadth of the 57-Å phase spots indicates a very short range positional correlation between layers. It is noted that the maximum intensity of the inner spots corresponds to $2\pi/Q$ = 53 Å instead of the Bragg value of 57 Å. This indicates that the molecular form factor increases with increasing Q in this region of reciprocal space. By contrast, in samples slowly cooled from the 41-Å phase the reflections of the 57-Å phase are reasonably sharp and close to their proper Bragg positions.

A series of radial densitometer scans of a fiber pattern covering the region of intermediate and wide angles is shown in Figure 9. In the lower angle region (left) the equatorial scans show, in the order of increasing Q: (1) the sharp first-order peak of the 32-Å phase, (2) the broad third-order peak (19 Å) of the 57-Å phase with a shoulder (3) at 16 Å due to the second-order reflection of the 32 Å phase, and (4) the fifth-order peak (11.5 Å) of the 57-Å phase. The wide-angle diffuse halo (the right-hand side of Figure 9) shows four pronounced maxima situated approximately halfway between the equator and the meridian.

Heating the fiber above 120 °C converts both the 57-Å and the 32-Å phase into a single 41-Å phase. In our experiment with the fiber the layer reflection from the 41-Å phase remained partly at the equator but partly it moved to the meridian, giving a four-arc pattern. Since this experiment had to be performed with the fiber supported within the glass capillary, surface alignment may have played a role in this partial reorientation. However, it is interesting to note that on subsequent slow cooling an overall reorientation to the four SAXS arcs took place, resulting again in four sharp arcs of the first and third order of the 57-Å phase, but this time with an inclination of approximately 45° to the original equatorial/meridional ones.

Finally, diffraction patterns were also recorded with the beam parallel to the fiber axis. The patterns revealed close to perfect cylindrical symmetry. Measurements of asimuthal intensity distribution in cases where there was some departure from perfect cylindrical symmetry showed that the distribution was the same for different diffraction orders of a given phase. This finding provided further confirmation that the assignment of the individual reflections as 001 smectic reflections was correct.

The present first X-ray scattering study of a crown ether substituted liquid crystal polymer reveals a complex phase behavior in this system. We have demonstrated the existence of a nematic and three smectic phases with different chain packings and different mobilities. These findings add to the prospect of potential application of this type of polymer for ion- or molecule-selective devices that may be controlled by regulating the temperature or the external field.

Regarding the nematic phase, the present work has confirmed the validity of our previous tentative assignment, which was based only on optical and calorimetric evidence.[10] Moreover, it is shown here that nematic glass can be produced at room temperature by precipating the PMC-11 polymer from solution.

In what follows the smectic phases will be discussed in more detail with special reference to their relative stabilities and possible structural models. A more comprehensive structural analysis will be published separately.

Thermal Behavior and Stability of Smectic Phases. Previous work[10] using optical microscopy and DSC suggested the existence of one smectic phase in PMC-11 and two smectic phases in the analogous polymer PSC-11, which has a siloxane backbone. These original suggestions were largely based on the fact that heating a PMC-11 polymer into the nematic phase produces one DSC endotherm (Figure 1), while heating the PSC-11 polymer produces two endotherms.[10] Now that three smectic phases have been recognized in PMC-11, it would be interesting to establish whether there are more than two smectic phases in the siloxane polymer and whether the phases involved are of the same type as those found here.

Of these three smectic phases in PMC-11, two appear to be stable and one metastable. The stable forms are the 57-Å phase, up to approximately 125 °C, and the 41-Å phase, between 125 °C and approximately 132 °C. That the 57-Å form is the genuinely stable low-temperature form, and not merely a kinetically favored variant, has been demonstrated by the fact that the 41-Å form transforms into the 57-Å phase provided the polymer is cooled sufficiently slowly. It is in fact the 32-Å form that, though less stable, is kinetically favored over the 57-Å form and on rapid cooling the 41-Å form will convert into

the 32-Å phase almost quantitatively. The fact that the 41-Å form has never been observed at room temperature and that the 32-Å reflection is always sharp suggests that the 41- and 32-Å forms are structurally closely related so that the transformation is "easy" and does not involve a major molecular rearrangement.

On the contrary, the 41 to 57 Å transformation is very sluggish and the diffraction peaks of the 57-Å phase are generally broad indicating an imperfect structure with a short correlation length. This would suggest that a major molecular rearrangement must take place during the transition. It is further noted that the 57-Å phase lacks the ability to perfect appreciably on annealing event at temperatures close to the upper end of its stability range. This would suggest a rather rigid structure, and the 57-Å phase may possibly be described more appropriately as smectic glass rather than a smectic liquid crystal.[20] In this context it should be recalled that the viscosity drops markedly upon the 57 to 41 Å phase change. The rigidity of the 57-Å phase may possibly be traced to a molecular rearrangement with strong electrostatic interactions between the crown ether moieties.

Structural Models. First of all it should be reiterated that for the wide-angle range only diffuse scattering is observed for all PMC-11 phases. Consequently all three smectic phases observed fall in the smectic A or smectic C category. Thus, for futher structural details we have to rely essentially on whatever information is contained in the 001 layer reflections.

Most proposed structures of smectic polymers so far have been based on building molecular models and comparing them with the observed layer periodicity from the position of 001 reflections. Scattering intensity data have generally not been utilized, except in only a few cases,[21,22] and thus a considerable degree of uncertainty accompanies many of the proposed models. We have chosen to utilize the intensity data and have adopted the approach of Richardson et al.[23] for monolayer smectics. The method is described here only briefly and the full account will be reported elsewhere. We first build the most probable model of the monomer unit (referred to here as the "molecule"), find the long axis of inertia and call it the director, and create the second molecule by inverting the first one and shifting it along the director by a variable parameter Δ. Additionally, if the measured layer periodicity is less than the length of the molecule, the director is appropriately tilted with respect to the layer normal. The one-dimensional structure factor is then calculated for such a "unit cell" by Fourier synthesis. Its squared values at the discrete 001 points in reciprocal space, F^2_{001}, are then plotted as a function of the shift Δ and a comparison with observed relative intensities i_{001} is made. The values of i_{001} are Lorentz-corrected intregral intensities measured on unoriented samples. The method also has provision for varying the orientational order parameter P_2 of the director, and we utilize this option to test whether the $F^2_{00_R}$ values for a suitable choice of Δ vary substantially within a reasonable range of P_2 values.

As for the different smectic phases in PMC-11 it should be said at the outset that, so far, we only have a satisfactory model for the 41-Å phase. Since the length of our model side chain, including the corresponding backbone segment and the van der Walls radii (Figure 2), turns out to be exactly 41 Å, it is most improbable that the 41-Å phase is anything but a straightforward monolayer smectic A phase. Note that many side-chain smectic polymers have a double-layer structure with the observed 001 periodicity twice the side-chain length.[24,25] This arises from a head-to-head arrangement of the side groups with the backbones separated by two layers of mesogens. Here this is clearly not the case: the backbones are separated by only one layer of mesogens and we can calculate the form factor of the layer according to the procedure described above.

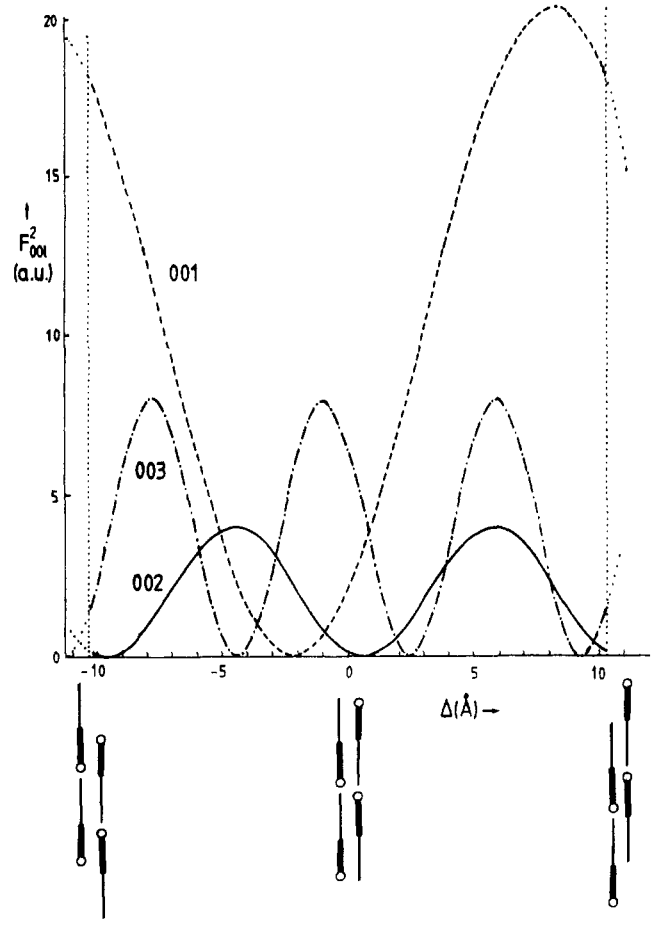

Figure 10. Calculated dependence of the squared one-dimensional structure factor F^2_{001} for a model PMC-11 layer as a function of Δ. Δ is the amount (in Å) by which a monomer is shifted along the layer normal with respect to the origin. A shift by Δ results in a relative displacement of two inverted monomers by 2Δ. Values for F^2 are shown at reciprocal lattice points 001 (- - -), 002 (—), and 003 (- · -). The relative positions of four monomer units in two adjacent horizontal layers are schematically shown at the bottom for $\Delta = -L/4$, $\Delta = 0$, and $\Delta = +L/4$ (note that the arrangements for $\Delta = -L/4$ and $\Delta = +L/4$ are indistinguishable).

Only two packing arrangements in the $L = 41$ Å phase, i.e., two fairly narrow ranges of Δ-values, turn out to be compatible with the observed diffraction intensities. This becomes clear from an inspection of Figure 10, where the values of the squared structure factor, F^2_{001}, are plotted as a function of the molecular shift Δ, at the reciprocal lattice points 001, 002, and 003. For symmetry reasons only the region $-L/4 < \Delta < +L/4$ (i.e., -10.25 Å $< \Delta <$ $+10.25$ Å) need be considered. It can be seen that only in the two limited regions around $\Delta = 2.5$ Å and $\Delta = 9$ Å the condition $F^2_{001} > F^2_{002} > F^2_{003}$ is fulfilled. The corresponding molecular packings are depicted in parts a and b of Figure 11. Other arrangements would all give relative intensities of 001 reflections that would qualitatively conflict with the observed ones. In particular, either 002 or 003 reflections would be more intense than 001 or else 003 would be significantly stronger than 002. For Δ values other than 2.5 and 9 Å, even taking account of the translational disorder (Debye–Weller factor) could not reconcile the large discrepancies between calculation and the observation of an intense 001, a weak 002, and no

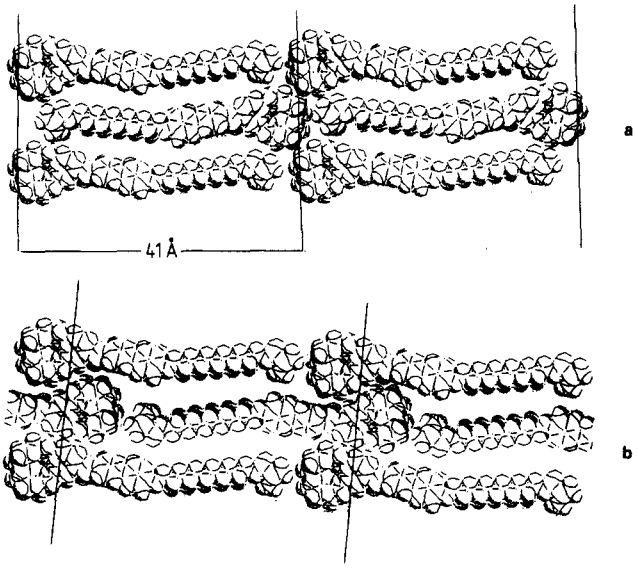

Figure 11. Two possible models of the 41-Å phase, both qualitatively compatible with the observed relative diffraction intensities: (a) shift $\Delta = 2.5$ Å, (b) $\Delta = 9$ Å. The models shown do not imply the existence of long-range order in alternating monomer orientations.

visible 003 reflection. Unfortunately, at the present time we are not in a position to say which of the two molecular arrangements in Figure 11 is the right one. Both have similar fairly low packing densities, particularly in the region of the alkyl part of the side chain. Low density seems inevitable with such bulky heterocyclic groups and only a tilt of the side chains would remedy the situation to some extent. It appears that the chains are indeed tilted in the two low-temperature phases (see below). Note that in both parts a and b of Figure 11 the backbone parts of the monomer units are staggered rather than lying in the same plane. However, in the model in Figure 11a staggering is less serious, which means that two side groups protruding into different adjacent layers, i.e., one pointing to the left and the other to the right in Figure 11, could still be emanating from the same backbone. This is difficult to envisage with the model in Figure 11b, so that the above consideration makes the arrangement in Figure 11a a little more likely.

The low-temperature metastable 32-Å phase has not yet been analyzed in quantitative detail. It is again clearly a monolayer phase, but it involves chain tilt. If the side chain as a whole is tilted, the angle would be 40°. Note that the transition between the 41- and 32-Å phases is discontinuous, unlike the normal smectic A–smectic C transition, which is second order.

Finally, the 57-Å phase proves to be more complex than initially suspected and at present we do not have a satisfactory model. Further study of this phase is in progress. At first sight it is tempting to interpret it as an interdigitated smectic A phase where either the flexible (spacer and backbone) or the rigid parts (biphenyl and benzocrown) overlap. This model would be consistent with the observed periodicity (57 Å) being close to 1.5 times the length of the extended side group. Note that the monomer unit consists of two parts of nearly equal length: the rigid part, 21.5 Å, and the flexible part, 19.5 Å. However, no model based on orthogonal layers could be made to even approximately match the observed diffraction intensities. We recall that only odd 001 orders are seen with $l = 1$, 3, and 5 and that the corrected intensity of the 003 reflection is four times that of the 001 reflection. Already a qualitative consideration would suggest that, since even orders are fully or almost fully extinct, a complete 57-Å layer probably consists of two sublayers of equal thickness and different densities. Alternatively, a similar symmetrical variant could be envisaged. However, such a situation would not be realized in an interdigitated smectic A structure described above since the thickness ratio of the two sublayers would in that case be close to 2:1 rather than 1:1. A more complex structure with fully or partially tilted side groups is thus more likely to be found in the 57-Å phase. There are two additional indications that chain tilt is involved. One is the already mentioned observation that the orientation of the 001 arcs in a partially oriented sample changes upon the 41 to 57 Å phase transition. the other is the appearance of four diffuse WAXS maxima halfway between the equator and the meridian (Figure 9) in the fiber pattern.

Conclusions

The present is the first structural study of a crown ether substituted liquid crystalline polymer. The main conclusions are as follows: (1) It is confirmed that the high-temperature anisotropic phase between 132 and 166 °C is nematic. (2) Three different smectic phases are observed below this range: (a) a high-temperature phase, stable between approximately 125 and 132 °C, with a layer periodicity $L = 41$ Å, (b) a low-temperature phase stable below 125 °C with $L = 57$ Å, and (c) a low-temperature metastable phase with $L = 32$ Å. (3) The 41-Å phase is a monolayer smectic A phase of low viscosity. Calculation of the layer form factor and a comparison with observed 001 diffraction intensities leave only two possible molecular arrangements. The one that appears more likely has mesogen and spacer moieties on neighboring side chains in juxtaposition (Figure 10a). (4) The 57-Å form is also a smectic phase with intralayer disorder but with high viscosity. Its structure is not yet understood but it appears to have tilted side groups and is a partially or fully double-layer phase. (5) The metastable 32-Å phase is a tilted variant (smectic C type) of the 41-Å phase and it too has high viscosity. It is kinetically favored over the 57-Å phase. (6) The bulkiness of the heterocyclic groups and ther specific interactions appear to cause unusual phase behavior, such as (a) a very low rate of transformation between the 41- and 57-Å smectic phases and (b) a highly discontinuous smectic C to smectic A transition.

Further work on a more detailed structural characterization is in progress.

Acknowledgment. We are indebted to Dr. R. M. Richardson of Bristol University for a helpful discussion and for providing the computer programs for molecular form factor calculations. The use of some of the experimental facilities of the Physics Department of Bristol University is acknowledged and our thanks are due to Professors A. Keller and E. D. T. Atkins. The financial support of this work by the National Science Foundation, Polymers Program (DMR-86-19724), is also acknowledged.

References and Notes

(1) Lehn, J. M. *Angew. Chem., Int. Ed. Engl.* **1988**, *27*, 89.
(2) Cram, D. J. *Angew. Chem., Int. Ed. Engl.* **1988**, 27, 1009.
(3) Pedersen, C. J. *Angew. Chem., Int. Ed. Engl.* **1988**, *27*, 1021.
(4) He, G. X.; Wada, F.; Kikukawa, K.; Masuda, T. *J. Chem. Soc., Chem. Commun.* **1987**, 1294.
(5) He, G.; Wada, F.; Kikukawa, K.; Shinkai, S.; Matsuda, T. *J. Org. Chem.* **1990**, *55*, 541.
(6) He, G.; Wada, F.; Kikukawa, K.; Shinkai, S.; Matsuda, T. *J. Org. Chem.* **1990**, *55*, 548.
(7) Lehn, J. M.; Malthete, J.; Levelut, A. M. *J. Chem. Soc., Chem. Commun.* **1985**, 1794.

(8) Mertesdorf, C.; Ringsdorf, H. *Liq. Cryst.* **1989**, *5*, 1757.
(9) Percec, V.; Rodenhouse, R. *Macromolecules* **1989**, *22*, 2043.
(10) Percec, V.; Rodenhouse, R. *Macromolecules* **1989**, *22*, 4408.
(11) Percec, V.; Rodenhouse, R. *J. Polym. Sci., Part A: Polym. Chem.* **1981**, *29*, 15.
(12) Rodenhouse, R.; Percec, V.; Feiring, A. E. *J. Polym. Sci., Part C: Polym. Lett.* **1990**, *28*, 345.
(13) Rodenhouse, R.; Percec, V. *Adv. Mater.* **1981**, *3*, 101.
(14) Hanson, I. R. *Acta Crystallogr.* **1978**, *B34*, 1026.
(15) Hummel, J. P.; Flory, P. J. *Macromolecules* **1980**, *13*, 479.
(16) Schmid, E. D.; Brosa, B. *J. Chem. Phys.* **1972**, *56*, 6267.
(17) d'Annibale, A.; Lunazzi, L.; Boicelli, A. C.; Macciantelli, D. *J. Chem. Soc., Perkin Trans. 2* **1973**, 1396.
(18) Bryan, R. F.; Hartley, P.; Miller, R. W.; Shen, M. S. *Mol. Cryst. Liq. Cryst.* **1980**, *62*, 281.
(19) Percec, V.; Hahn, B.; Ebert, M.; Wendorff, J. H. *Macromolecules* **1990**, *23*, 2092.
(20) Wunderlich, B.; Moller, M.; Grebowicz, J.; Baur, H. *Adv. Polym. Sci.* **1988**, *87*, 1.
(21) Gudkov, V. A.; Chistyakov, I. G.; Shibaev, V. P.; Vainshtein, B. K. *Sov. Phys. Crystallogr.* **1982**, *27*, 324.
(22) Gudkov, V. A. *Sov. Phys. Crystallogr.* **1987**, *31*, 686.
(23) Richardson, R. M.; Leadbetter, A. J.; Mazid, M. A.; Tucker, P. A. *Mol. Cryst. Liq. Cryst.* **1987**, *149*, 329.
(24) Shibaev, V. P.; Plate, N. A. *Adv. Polym. Sci.* **1984**, *60/61*, 173.
(25) Richardson, R. M.; Herring, N. J. *Mol. Cryst. Liq. Cryst.* **1985**, *123*, 147.